

Hyperfine structure of antiprotonic helium energy levels

D. Bakalov*

Institute for Nuclear Research and Nuclear Energy, Sofia 1784, Bulgaria

V. I. Korobov†

Joint Institute for Nuclear Research, 141980, Dubna, Russia

(Received 30 July 1997)

We present a theoretical calculation of the fine and hyperfine splittings of the energy levels in the metastable states of antiprotonic helium ${}^4\text{He}^+p^-$, performed with the accuracy of 10^{-4} . We also discuss the perspectives of obtaining experimental data on the magnetic moment of the antiproton from measurements of the hyperfine structure of antiprotonic helium. [S1050-2947(98)02802-9]

PACS number(s): 36.10.-k, 31.15.Ar

I. INTRODUCTION

Spectacular progress has been achieved recently in the spectroscopy of antiprotonic helium [1–5]. On the one hand, Yamazaki *et al.*, Morita *et al.*, Hayano *et al.*, and Maas *et al.* have succeeded in measuring the wavelengths of several transitions between various metastable states with an accuracy of 5×10^{-6} . On the other hand, the Coulomb energy levels of the antiprotonic helium atom have been calculated with an accuracy 10^{-7} [6]. By subsequently taking into account the leading-order QED and relativistic corrections, the discrepancy between theory and experiment has been reduced to only 5–10 ppm [7]. While this remarkable agreement has provided a most convincing confirmation of the Condo model [8] of the phenomenon of delayed annihilation of antiprotons in helium [9], the projects to measure experimentally the fine and hyperfine structure of antiprotonic helium atoms in the upcoming years [10] are making way for frontier tests of QED.

We present in this paper the theoretical results for the fine and hyperfine splittings of the metastable energy levels of antiprotonic helium atoms, accurate to 10^{-4} . The hyperfine structure of antiprotonic helium has already been observed experimentally [10] and the experiments that are now being prepared are expected to boost significantly the accuracy of the measurements. The situation will become particularly exciting if the experimental precision reaches 10^{-4} since the data would then provide valuable information on the electromagnetic structure of antiprotons and eventually an opportunity to test *CPT*.

II. THEORETICAL CONSIDERATIONS

A. Three-body Hamiltonian

The antiprotonic helium atoms consist of a helium nucleus, an electron, and an antiproton. According to the Condo model, they are formed when the antiprotons, after being slowed down in helium, are captured by helium atoms

in highly excited bound states with a nearly circular antiprotonic orbital. Our quantum-mechanical approach to this particular three-body problem is based on the three-body relativistic Hamiltonian, derived in [11,12] within the instant form of directly interacting particle dynamics [13,14].

In first order of perturbation theory the fine and hyperfine splittings of the energy levels are due uniquely to interactions that explicitly involve particle spin operators s_i . [The radiative corrections to the Coulomb potential that contribute by quantities of $O(\alpha^5 \ln \alpha)$ to the fine splitting of hydrogen *shift* the atomic levels rather than splitting them.] Up to terms of $O(\alpha^4)$ the interaction part of the three-body relativistic Hamiltonian of [11,12] U has the form of a sum of pairwise Breit interaction operators, calculated in the one-photon-exchange approximation

$$U = U_{12} + U_{13} + U_{23}.$$

We keep in U_{ij} only those terms that explicitly involve s_i , denote by \mathbf{r}_i , \mathbf{p}_i , m_i , z_i , and $\boldsymbol{\mu}_i$ the position vector of the i th particle, its momentum, its mass, electric charge (in units $|e|$), and magnetic dipole moment (in units $e\hbar/2m_i c$) and also set $\mathbf{r} = \mathbf{r}_j - \mathbf{r}_i$. In atomic units $e = \hbar = 1$ we have, for the interaction of a pair of spin-1/2 particles,

$$\begin{aligned} U_{ij} = \alpha^2 \left\{ -\frac{8\pi}{3} \left(\frac{\boldsymbol{\mu}_i}{m_i} \right) \left(\frac{\boldsymbol{\mu}_j}{m_j} \right) (\mathbf{s}_i \cdot \mathbf{s}_j) \delta(\mathbf{r}) \right. \\ - \frac{1}{r^5} \left(\frac{\boldsymbol{\mu}_i}{m_i} \right) \left(\frac{\boldsymbol{\mu}_j}{m_j} \right) [3(\mathbf{r} \cdot \mathbf{s}_i)(\mathbf{r} \cdot \mathbf{s}_j) - r^2(\mathbf{s}_i \cdot \mathbf{s}_j)] \\ - (z_i - 2\mu_i) \frac{z_j}{2m_i^2 r^3} (\mathbf{r} \times \mathbf{p}_i) \cdot \mathbf{s}_i + \frac{z_i \mu_j}{m_i m_j r^3} (\mathbf{r} \times \mathbf{p}_i) \cdot \mathbf{s}_j \\ \left. + (z_j - 2\mu_j) \frac{z_i}{2m_j^2 r^3} (\mathbf{r} \times \mathbf{p}_j) \cdot \mathbf{s}_j - \frac{z_j \mu_i}{m_i m_j r^3} (\mathbf{r} \times \mathbf{p}_j) \cdot \mathbf{s}_i \right\}. \end{aligned} \quad (1)$$

and for the interaction of a spin-1/2 particle with a spinless one,

*Electronic address: dbakalov@inrne.acad.bg

†Electronic address: korobov@nu.jinr.dubna.su

$$U_{ij} = -\alpha^2 \left\{ (z_i - 2\mu_i) \frac{z_j}{2m_i^2 r^3} (\mathbf{r} \times \mathbf{p}_i) \cdot \mathbf{s}_i + \frac{z_j \mu_i}{m_i m_j r^3} (\mathbf{r} \times \mathbf{p}_j) \cdot \mathbf{s}_i \right\}. \quad (2)$$

It is worth discussing briefly the accuracy of U . The pairwise spin interaction U_{ij} does not include terms of order higher than $O(\alpha^4)$; however, the only contribution of $O(\alpha^5)$, related to the anomalous magnetic moment of the particles, has been incorporated in the phenomenological value of the total magnetic moment μ_i [15], so that the inaccuracy of U_{ij} is of $O(\alpha^6)$. The lowest-order three-body interaction terms appearing in the Foldy-Krajcik scheme [14] are also $O(\alpha^6)$ since the Foldy-Krajcik Hamiltonian has the form of a series in $1/c^2 = \alpha^2$. Therefore, the spin interaction Hamiltonian of Eqs. (1) and (2) is accurate to $O(\alpha^6)$, which exceeds the accuracy of the Dirac equation for the particular case of antiprotonic helium by an order of magnitude.

B. Perturbative calculation of the level splitting

The classification of the eigenstates of three-body systems of scalar particles requires a set of six quantum numbers (QNs), e.g., the values of the total orbital moment l and its projection on the fixed frame z axis M (both of them exact QNs) plus four approximate QNs that are traditionally associated with the vibrational excitations of particles 1 and 2 and to the motion of the third particle around them; of course, the spatial parity λ is also conserved. In the particular case of antiprotonic helium metastable states, the third particle, the electron, is always in the ‘‘ground state’’ and the energy levels are labeled with l and the ‘‘radial’’ excitation QN n_r or, alternatively, by the ‘‘principal’’ QN $n = n_r + l + 1$ and l . Things change if particle spins are taken into account: the orbital moment l now couples to the electron spin s_3 to produce the intermediate moment $\mathbf{J} = \mathbf{l} + \mathbf{s}_3$ (which is quite a ‘‘good’’ QN because of the dominance of the electron spin-orbital interaction); in turn \mathbf{J} couples to the antiproton spin s_2 to give the total angular moment $\mathbf{F} = \mathbf{J} + \mathbf{s}_2$ (exactly conserved together with its projection F_z). The energy levels E^{nJF} differ from the corresponding purely Coulombic energy levels E^{nl} by a correction term ΔE^{nJF} , attributed to the spin interaction Hamiltonian U : $E^{nJF} = E^{nl} + \Delta E^{nJF}$; the fine splitting is associated with the dependence of the energy levels on J , while the hyperfine splitting is associated with the F dependence.

The initial zeroth order approximation for the spin-dependent wave function of the antiprotonic helium atom is

$$\psi^{nJFF_z}(\mathbf{R}, \mathbf{r}) = \sum_{J'} \beta_{J'}^{nJF} |nJ'FF_z\rangle, \quad (3)$$

$$|nJ'FF_z\rangle = \sum_{\xi_2, \xi_3, M, J'_z} C_{lM, s_3 \xi_3}^{J'J'_z} C_{J'J'_z, s_2 \xi_2}^{FF_z} \times \Psi^{nIM}(\mathbf{R}, \mathbf{r}) |s_2 \xi_2\rangle |s_3 \xi_3\rangle,$$

where C are Clebsch-Gordan coefficient, $|s \xi\rangle$ are constant spinors, β are constant amplitudes (to be calculated from the

secular equation), and Ψ is the three-body Coulomb wave function, expressed in terms of the Jacobi coordinates of the particles \mathbf{R}, \mathbf{r} , as calculated in [6]:

$$\Psi^{nIM}(\mathbf{R}, \mathbf{r}) = \sum_{m=0}^l \mathcal{D}_{Mm}^{nI}(\Phi, \Theta, \varphi) F_m^{nI}(R, \xi, \eta). \quad (4)$$

Here \mathcal{D}_{Mm}^{nI} are the symmetrized Wigner functions of parity $\lambda = (-1)^l$. The components $F_m^{nI}(R, \xi, \eta)$ of the variational wave function are taken in the form

$$F_m^{nI}(R, \xi, \eta) = R^m [(\xi^2 - 1) \times (1 - \eta^2)]^{m/2} R^{l*} \sum_{i=1}^N c_i R^{i_t} \xi^{j_i} \eta^{k_i} e^{-(\alpha + \beta \xi)R}, \quad (5)$$

where $\xi = (R_1 + R_2)/R$ and $\eta = (R_1 - R_2)/R$ are the prolate spheroidal coordinates of the electron, $i_t \geq j_t$, and the factor R^{l*} is introduced to meet the requirement that the antiproton is on a nearly circular orbit.

We restrict ourselves to first order of perturbation theory because the calculation of the effects of the spin interaction U in higher orders makes little sense if other terms of the same order of magnitude have been omitted and also because the use of the singular operators in Eqs. (1) and (2) beyond perturbation theory is not mathematically justified. In first order of perturbation theory the spin corrections to the energy levels ΔE^{nJF} and the amplitudes $\beta_{J'}^{nJF}$ are, respectively, the eigenvalues and eigenvectors of the spin interaction matrix in the representation of Eq. (3):

$$\sum_{J'} (\langle nJF | U | nJ'F \rangle - \Delta E^{nJF} \delta_{JJ'}) \beta_{J'}^{nJF} = 0. \quad (6)$$

The calculation of the spin interaction matrix involves integration over \mathbf{R}, \mathbf{r} and summation over the spinor variables. The intermediate results of the averaging of U over the spatial variables can be represented in the form of an ‘‘effective spin Hamiltonian’’ H^{eff} . By definition, H^{eff} is an operator in the finite-dimensional space of the direct product of the representations $(l) \otimes (s_2) \otimes (s_3)$ of $\text{su}(2)$, such that its matrix elements coincide with the spin interaction matrix defined earlier:

$$(lJFF_z | H^{\text{eff}} | lJ'FF_z) = \langle nJFF_z | U | nJ'FF_z \rangle,$$

where, unlike $|nJ'FF_z\rangle$ in Eq. (3), the state vector $|lJ'FF_z\rangle$ is built up out of constant spinors only:

$$|lJFF_z\rangle = \sum_{\xi_2, \xi_3, J_z, M} C_{lM, s_3 \xi_3}^{JJ_z} C_{JJ_z, s_2 \xi_2}^{FF_z} |lM\rangle |s_2 \xi_2\rangle |s_3 \xi_3\rangle.$$

The effective spin Hamiltonian is a compact way to represent the results of the quite nontrivial numerical integration over the spatial variables in terms of a few constants. In the particular case of antiprotonic helium H^{eff} has the form

$$H^{\text{eff}} = E_1(\mathbf{s}_3 \cdot \mathbf{l}) + E_2(\mathbf{s}_2 \cdot \mathbf{l}) + E_3(\mathbf{s}_2 \cdot \mathbf{s}_3) + E_4 \{ 2l(l+1)(\mathbf{s}_2 \cdot \mathbf{s}_3) - 3[(\mathbf{s}_2 \cdot \mathbf{l})(\mathbf{s}_3 \cdot \mathbf{l}) + (\mathbf{s}_3 \cdot \mathbf{l})(\mathbf{s}_2 \cdot \mathbf{l})] \}. \quad (7)$$

TABLE I. Coefficients of the effective spin Hamiltonian H^{eff} of Eq. (7), for the range of states of $\bar{p}^4\text{He}^+$ with $31 \leq l \leq 38$ and $l+1 \leq n \leq l+5$ (in a.u.). Numbers in square brackets indicate powers of 10.

(n, l)	E_1	E_2	E_3	E_4
(32,31)	-0.706761[-7]	0.186755[-8]	-0.767867[-7]	-0.108287[-10]
(33,31)	-0.669560[-7]	0.164319[-8]	-0.686551[-7]	-0.113463[-10]
(34,31)	-0.626303[-7]	0.144741[-8]	-0.606467[-7]	-0.116717[-10]
(35,31)	-0.587130[-7]	0.127225[-8]	-0.535116[-7]	-0.118388[-10]
(33,32)	-0.684561[-7]	0.148425[-8]	-0.709382[-7]	-0.106521[-10]
(34,32)	-0.644394[-7]	0.130323[-8]	-0.628579[-7]	-0.110325[-10]
(35,32)	-0.600444[-7]	0.114521[-8]	-0.553117[-7]	-0.112110[-10]
(36,32)	-0.555291[-7]	0.101201[-8]	-0.477244[-7]	-0.111748[-10]
(37,32)	-0.512013[-7]	0.881481[-9]	-0.416257[-7]	-0.110799[-10]
(34,33)	-0.659821[-7]	0.117790[-8]	-0.649376[-7]	-0.104344[-10]
(35,33)	-0.616417[-7]	0.103173[-8]	-0.569628[-7]	-0.106717[-10]
(36,33)	-0.571004[-7]	0.903227[-9]	-0.495197[-7]	-0.107250[-10]
(37,33)	-0.524598[-7]	0.790858[-9]	-0.427290[-7]	-0.106029[-10]
(38,33)	-0.475612[-7]	0.696419[-9]	-0.365270[-7]	-0.102946[-10]
(35,34)	-0.632310[-7]	0.932232[-9]	-0.588143[-7]	-0.101698[-10]
(36,34)	-0.585778[-7]	0.814351[-9]	-0.510324[-7]	-0.102611[-10]
(37,34)	-0.538136[-7]	0.711276[-9]	-0.439222[-7]	-0.101729[-10]
(38,34)	-0.490675[-7]	0.621686[-9]	-0.375766[-7]	-0.992305[-11]
(39,34)	-0.444559[-7]	0.544291[-9]	-0.320383[-7]	-0.953829[-11]
(36,35)	-0.601839[-7]	0.734824[-9]	-0.526124[-7]	-0.985305[-11]
(37,35)	-0.552519[-7]	0.640123[-9]	-0.451341[-7]	-0.979852[-11]
(38,35)	-0.503192[-7]	0.557945[-9]	-0.384595[-7]	-0.957660[-11]
(39,35)	-0.455167[-7]	0.487128[-9]	-0.326436[-7]	-0.921270[-11]
(40,35)	-0.409674[-7]	0.426476[-9]	-0.276836[-7]	-0.874598[-11]
(37,36)	-0.568286[-7]	0.576101[-9]	-0.463858[-7]	-0.947854[-11]
(38,36)	-0.516768[-7]	0.500564[-9]	-0.393369[-7]	-0.928261[-11]
(39,36)	-0.466511[-7]	0.435656[-9]	-0.332082[-7]	-0.893855[-11]
(40,36)	-0.418844[-7]	0.380283[-9]	-0.280014[-7]	-0.848296[-11]
(41,36)	-0.374439[-7]	0.333282[-9]	-0.236650[-7]	-0.794519[-11]
(38,37)	-0.531644[-7]	0.448636[-9]	-0.402067[-7]	-0.904184[-11]
(39,37)	-0.478774[-7]	0.389050[-9]	-0.337226[-7]	-0.871397[-11]
(40,37)	-0.428577[-7]	0.338451[-9]	-0.282440[-7]	-0.826581[-11]
(41,37)	-0.382130[-7]	0.295747[-9]	-0.237124[-7]	-0.773870[-11]
(42,37)	-0.337968[-7]	0.259496[-9]	-0.200235[-7]	-0.710391[-11]
(39,38)	-0.492063[-7]	0.346618[-9]	-0.341654[-7]	-0.853995[-11]
(40,38)	-0.438953[-7]	0.300354[-9]	-0.283814[-7]	-0.809582[-11]
(41,38)	-0.389982[-7]	0.261573[-9]	-0.236406[-7]	-0.756816[-11]
(42,38)	-0.344785[-7]	0.229034[-9]	-0.198221[-7]	-0.696576[-11]
(43,38)	-0.293643[-7]	0.199726[-9]	-0.167784[-7]	-0.602641[-11]

The values of E_1, \dots, E_4 for the whole range of excited $\bar{p}^4\text{He}^+$ states of interest are listed in Table I. The value of the magnetic moment of the antiproton was taken to be exactly the opposite of the protonic magnetic moment: $\mu_{\bar{p}} = -2.79285(e\hbar/2m_{\bar{p}}c)$.

III. SPIN EFFECTS IN ANTIPROTONIC HELIUM SPECTROSCOPY

We present in this section the numerical results of our calculation of the hyperfine structure of antiprotonic helium.

Having in mind the future spectroscopy experiments, we pay particular attention to the different possibilities of testing the theoretical predictions.

A. Hyperfine structure of the energy levels

Calculating the fine and hyperfine splittings ΔE^{nIJF} of the energy levels of the antiprotonic helium atom and the corresponding spin state vector $\beta_{J'}^{nIJF}$ from Eq. (6) is straightforward. In particular, for $F = l \pm 1$ we simply have

TABLE II. Fine and hyperfine splittings, ΔE^{nJJF} (in gigahertz), of the nonrelativistic energy levels of the antiprotonic helium atom $\bar{p}^{-4}\text{He}^{+}$ and mixing parameter ϕ for the range of states with $31 \leq l \leq 38$ and $l+1 \leq n \leq l+5$.

(n, l)	JF				ϕ
	$(l+1/2, l+1)$	$(l+1/2, l)$	$(l-1/2, l)$	$(l-1/2, l-1)$	
(32,31)	-7.0764	-7.3507	7.6884	7.1916	-0.0219
(33,31)	-6.7033	-6.9644	7.2571	6.8405	-0.0215
(34,31)	-6.2669	-6.5175	6.7661	6.4211	-0.0211
(35,31)	-5.8725	-6.1123	6.3229	6.0401	-0.0207
(33,32)	-7.0965	-7.3268	7.6326	7.2316	-0.0209
(34,32)	-6.6769	-6.9000	7.1613	6.8312	-0.0205
(35,32)	-6.2172	-6.4335	6.6536	6.3849	-0.0201
(36,32)	-5.7437	-5.9559	6.1371	5.9214	-0.0197
(37,32)	-5.2924	-5.4952	5.6439	5.4751	-0.0195
(34,33)	-7.0686	-7.2667	7.5396	7.2224	-0.0199
(35,33)	-6.5985	-6.7937	7.0230	6.7682	-0.0195
(36,33)	-6.1068	-6.2989	6.4884	6.2872	-0.0192
(37,33)	-5.6049	-5.7925	5.9466	5.7910	-0.0189
(38,33)	-5.0753	-5.2581	5.3805	5.2614	-0.0187
(35,34)	-6.9889	-7.1642	7.4035	7.1598	-0.0190
(36,34)	-6.4682	-6.6433	6.8406	6.6511	-0.0186
(37,34)	-5.9357	-6.1095	6.2695	6.1254	-0.0183
(38,34)	-5.4063	-5.5765	5.7042	5.5976	-0.0180
(39,34)	-4.8929	-5.0579	5.1585	5.0815	-0.0178
(36,35)	-6.8535	-7.0131	7.2184	7.0395	-0.0181
(37,35)	-6.2846	-6.4455	6.6112	6.4784	-0.0178
(38,35)	-5.7169	-5.8769	6.0084	5.9130	-0.0175
(39,35)	-5.1654	-5.3219	5.4247	5.3590	-0.0172
(40,35)	-4.6441	-4.7950	4.8745	4.8315	-0.0171
(37,36)	-6.6588	-6.8081	6.9797	6.8575	-0.0172
(38,36)	-6.0477	-6.1985	6.3337	6.2494	-0.0169
(39,36)	-5.4530	-5.6023	5.7070	5.6525	-0.0167
(40,36)	-4.8902	-5.0355	5.1155	5.0834	-0.0165
(41,36)	-4.3673	-4.5063	4.5670	4.5509	-0.0164
(38,37)	-6.4026	-6.5457	6.6842	6.6111	-0.0164
(39,37)	-5.7585	-5.9021	6.0081	5.9651	-0.0162
(40,37)	-5.1486	-5.2896	5.3695	5.3486	-0.0160
(41,37)	-4.5857	-4.7214	4.7810	4.7757	-0.0158
(42,37)	-4.0521	-4.1794	4.2243	4.2281	-0.0158
(39,38)	-6.0843	-6.2236	6.3302	6.2992	-0.0157
(40,38)	-5.4208	-5.5588	5.6378	5.6288	-0.0155
(41,38)	-4.8105	-4.9441	5.0018	5.0079	-0.0153
(42,38)	-4.2490	-4.3753	4.4174	4.4323	-0.0152
(43,38)	-3.6171	-3.7279	3.7616	3.7754	-0.0153

$\beta_{J'}^{nJJF} = \delta_{JJ'}$, while for $F=l$ the amplitudes β can be parametrized with the single parameter ϕ : $\beta_{J'}^{nJJF} = \sin \phi$ for $J=l-1/2, J'=l+1/2$. The numerical results for ΔE^{nJJF} and ϕ are presented in Table II.

Table II shows that the leading spin effect in antiprotonic helium spectroscopy is the fine splitting of the levels, associated with the dependence on $J=l \pm 1/2$; the hyperfine splitting (the F dependence) is suppressed by a factor ~ 80 . This is due to the fact that the spin interaction Hamiltonian U of Eqs. (1) and (2) is dominated by the spin-orbital interaction of the electron [the term $E_1(\mathbf{I} \cdot \mathbf{s}_3)$ in Eq. (7)]. The relative

contribution of the various terms of H^{eff} can be easily estimated with the help of Table I by taking into account that, for $l \gg 1$, $\langle s_2 \cdot s_3 \rangle \sim 1$, $\langle \mathbf{I} \cdot \mathbf{s}_i \rangle \sim l$ and $\langle 2l(l+1)(s_2 \cdot s_3) - 3[(s_2 \cdot \mathbf{I})(s_3 \cdot \mathbf{I}) + (s_3 \cdot \mathbf{I})(s_2 \cdot \mathbf{I})] \rangle \sim l^2$.

Future microwave-induced-transition experiments, the preparation of which was announced in [10], are designed to measure directly the fine splitting of the levels of antiprotonic helium, i.e., the separation between the doublets of states with $J=l \pm 1/2$. No estimates of the expected accuracy are known, but it will hardly allow for measuring the hyperfine splitting. Note that the contribution to the fine splitting

TABLE III. Hyperfine structure of the spectral line for the transition (37,35)→(38,34): spin correction $\Delta E^{(nIJF)\rightarrow(n'l'J'F')} = \Delta E^{(n'l'J'F')} - \Delta E^{(nIJF)}$ to the transition frequency (in gigahertz) and probability of the individual hyperfine components.

(J,F)	(J',F')			
	(l'+1/2,l'+1)	(l'+1/2,l')	(l'-1/2,l')	(l'-1/2,l'-1)
(l+1/2,l+1)	0.8783 1			
(l+1/2,l)	1.0392 1/2l ²	0.8690 1-1/2l ²		
(l-1/2,l)	-12.017 1/2l ²	-12.188 o(l ⁻²)	-0.9070 1-1/2l ²	
(l-1/2,l-1)	-11.885 o(l ⁻²)	-12.055 1/2l ²	-0.7742 1/2l ²	-0.8808 1-1/l ²

from the terms that explicitly involve the magnetic moment of the antiproton is suppressed by two orders of magnitude.

B. Hyperfine structure of the transition lines

While in the nonrelativistic approximation of spinless particles E1 transitions between two bound states of the antiprotonic helium atom (nl)→(n'l'), l'=l±1 would be signaled by a single spectral line, the spin interactions split this line to 4×4=16 components, depending on which are the parent and daughter hyperfine states: E^{(nIJF)→(n'l'J'F')} = E^{n'l'J'F'} - E^{nIJF} = E_{nr}^{(nl)→(n'l')} + ΔE^{(nIJF)→(n'l'J'F')} with E_{nr}^{(nl)→(n'l')} = E^{n'l'} - E^{nl} and ΔE^{(nIJF)→(n'l'J'F')} = ΔE^{n'l'J'F'} - ΔE^{nIJF}. The energy (and, respectively, the frequency) of each of these transitions can easily be calculated from the content of Table II. It is easy to notice that the spin corrections ΔE^{(nIJF)→(n'l'J'F')} to the “main” transitions between states with ΔF=ΔJ=Δl are suppressed because the corresponding corrections to the energy of the parent and daughter states cancel each other, but become quite significant in “crossed” transitions. Unfortunately (from the experimenter’s point of view), the probability for the crossed transitions is suppressed compared to the main ones. Consider in more detail the example of the transition (37,35)→(38,34) illustrated in Table III and Fig. 1. The rows of the table correspond to different initial states, while the columns refer to different final states. As long as E1 transitions with |ΔJ|>1 or |ΔF|>1 are strictly forbidden, their cells are empty; the other cells contain the fine and hyperfine splittings ΔE^{(nIJF)→(n'l'J'F')}, reckoned from the frequency of the nonrelativistic value E_{nr}^{(nl)→(n'l')} (upper row) and the relative probability of the various open channels for any of the initial states as a function of l (lower row). It is easy to see that the measurement of the splitting of the transition lines is a difficult task: either the separation of the sublines is too small to be observed (the four main lines) or their intensity is too strongly suppressed. What was reported in [10] was the measurement of the fine splitting between the main components with J=l+1/2 and J=l-1/2 (the upper and lower halves of the diagonal of Table III); the hyperfine splitting within them was not studied. Unfortun-

nately, these measurements, even further refined, would hardly bring new information on antiprotonic magnetic moment μ_{p̄} since the fine splitting of the main sublines is not sensitive enough to the value of μ_{p̄}: Changing its value by 0.5% would affect only the fifth digit of the splitting. Most suitable for measuring μ_{p̄} are the two components with ΔJ=1, ΔF=0, for which a change of 1% of its value shifts the transition frequency by 0.1%; the suppression factor for these components is 1/l²~10⁻³.

C. Discussion of the results

As pointed out in Sec. II, the interaction Hamiltonian does not include higher order QED terms that are expected to contribute by quantities of relative order 10⁻⁴ to the splitting ΔE^(nIJF), thus one strict upper limit of the precision follows from the choice of the theoretical model. The detailed study of the convergence of the numerical values of the coefficients of the effective spin Hamiltonian with respect to the number of basis functions in the variational expansion of Eq.

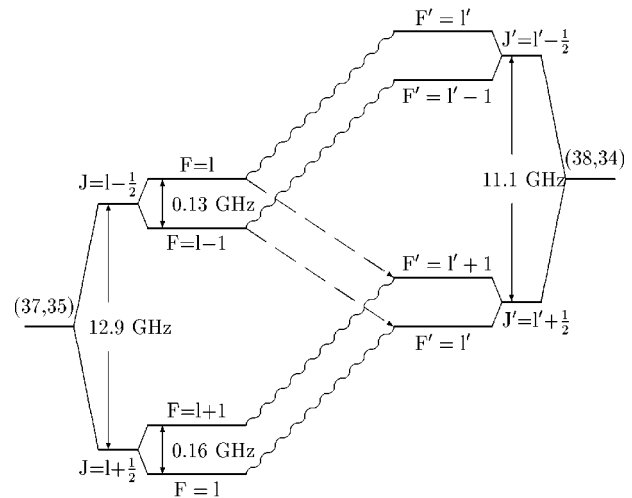


FIG. 1. Fine and hyperfine structure of the antiprotonic helium states (37,35) and (38,34) and the E1 transitions (37,35)→(38,34). The waved lines denote the main hyperfine components of the transition wavelength, while the dashed lines stand for the satellite wavelength suppressed by a factor of order 10⁻³.

TABLE IV. Convergence of the coefficients of the effective spin Hamiltonian E_i , $i=1, \dots, 4$ with respect to the number of basis functions in the variational expansion of Eq. (5). Numbers in square brackets indicate power of 10.

N	E_1	E_2	E_3	E_4
528	-0.552572[-7]	0.640388[-9]	-0.450603[-7]	-0.979187[-11]
880	-0.552471[-7]	0.640068[-9]	-0.451138[-7]	-0.979686[-11]
1728	-0.552411[-7]	0.640143[-9]	-0.451302[-7]	-0.979821[-11]
2364	-0.552519[-7]	0.640123[-9]	-0.451341[-7]	-0.979852[-11]

(5) demonstrates (see Table IV) that the numerical error does not exceed 10^{-4} either. Finally, the uncertainty of $\Delta E^{(nIJF)}$ due to the present uncertainty in the value of $\mu_{\bar{p}}$ is again $\sim 1.10^{-4}$. The conclusion, therefore, is that the overall uncertainty of the results on the fine and hyperfine splitting is not larger than 10^{-4} .

The comparison of the theoretical results of the present paper with the expected spectroscopic data from the future experiments will be a crucial test for the validity of the relativistic quantum mechanical approach to few-body problems involving antiparticles. If confirmed, this approach will have to be extended further to include the leading-order radiative correction in a way to provide results accurate to 10^{-5} . A comparison with experiment then would reduce the uncertainty in the experimental value -2.800 ± 0.008 (μ_N) of the

dipole magnetic moment of the antiproton [16] by an order of magnitude.

ACKNOWLEDGMENTS

The present work was supported by the NSF, Grant No. INT-9602189, which is gratefully acknowledged. D.B. is also grateful to the Bulgarian National Fund for Scientific Research for partial support under Grant No. FI-507. We are particularly indebted to Professor T. Yamazaki for many valuable suggestions and for his support at all the stages of the work, as well as to all the member of the CERN PS205 experiment group and to Profesor K. Szalewicz for the useful discussions.

-
- [1] T. Yamazaki *et al.*, Nature (London) **361**, 238 (1993).
 [2] N. Morita *et al.*, Phys. Rev. Lett. **72**, 1180 (1994).
 [3] R. S. Hayano *et al.*, Phys. Rev. Lett. **73**, 1485 (1994); **73**, 3181(E) (1994).
 [4] F Maas *et al.*, Phys. Rev. A **52**, 4266 (1995).
 [5] R. S. Hayano *et al.*, Phys. Rev. A **55**, R1 (1997).
 [6] V. I. Korobov, Phys. Rev. A **54**, 1749 (1996).
 [7] V. I. Korobov and D. Bakalov, Phys. Rev. Lett. **79**, 3379 (1997).
 [8] G. T. Condo, Phys. Lett. **9**, 65 (1964).
 [9] M. Iwasaki *et al.*, Phys. Rev. Lett. **67**, 1246 (1991).
 [10] E. Widmann *et al.*, Phys. Lett. B **404**, 15 (1997).
 [11] D. Bakalov, V. S. Melezhik, Phys. Lett. **161B**, 5 (1985).
 [12] D. Bakalov, Sov. J. Nucl. Phys. **48**, 210 (1988).
 [13] P. A. M. Dirac, Rev. Mod. Phys. **21**, 392 (1949).
 [14] L. Foldy and R. Krajcik, Phys. Rev. D **12**, 1700 (1975).
 [15] H. A. Bethe and E. E. Salpeter, *Quantum Mechanics of One- and Two-Electron Atoms* (Springer-Verlag, Berlin, 1957).
 [16] L. Montanet *et al.*, Phys. Rev. D **50**, 1173 (1994).